

Electromagnetic transitions of excited baryons in a deformed oscillator quark model

Atsushi Hosaka¹

Numazu College of Technology, Numazu, Shizuoka 410-8501, Japan

Miho Takayama² and Hiroshi Toki³

Research Center for Nuclear Physics (RCNP), Osaka University,
Ibaraki, Osaka 567-0047, Japan

Abstract

We study electromagnetic transitions of excited baryons in a deformed oscillator quark model, where baryon excited states are described as rotational bands of deformed intrinsic states. We describe all necessary tools to compute transition amplitudes in multipole basis, which are then related to the commonly used helicity amplitudes. We pay a special attention on the sign of the amplitudes as well as their absolute values by computing the photon and pion couplings simultaneously. We have found that the effect of deformation on the transition amplitudes is rather weak. The difficulty in reproducing the empirical amplitude of the Roper state is discussed.

¹e-mail address: hosaka@la.numazu-ct.ac.jp

²e-mail address: takayama@rcnp.osaka-u.ac.jp

³e-mail address: toki@rcnp.osaka-u.ac.jp

1 Introduction

Excited baryons as well as their ground states provide precious information on the dynamics of low energy QCD. Not only their masses but also various transitions are particularly important for the study of their structure and interactions. Recent and future experiments planned at facilities such as TJNAL, COSY, CELCIUS and SPring8 are aiming at obtaining more detailed information on hadron structure [1].

Based on conventional effective models of baryons, e.g., quark models, one can draw a simple but rather unified picture for both ground and excited states [2]. There, constituent quarks are placed in a confining potential and are interacting through suitable residual interactions. As a consequence, we have an intuitive picture similar to the atomic and nuclear physics; baryon states are described as single particle states of three valence quarks.

An extensive work was performed by Isgur and Karl in the non-relativistic (NR) quark model which has been applied to a variety of hadronic phenomena [3], including electromagnetic couplings of excited states [4]. Recently, the role of the Nambu-Goldstone bosons has been emphasized in the context of the chiral quark model [5]. In these models, important physics is dictated by valence quarks which are confined inside hadrons and interacting each other through residual interactions. In the Isgur-Karl model, one gluon exchanges are introduced, while in the chiral quark model flavor dependent forces generated by Nambu-Goldstone boson exchanges are included. These residual interactions yield hyper fine splittings in baryon masses with configuration mixing. In general, however, the quality of these models crucially depends on the type of residual interactions with considerable amount of parameters.

In such a situation, we still hope to find a better description for the entire baryonic system. In this respect, we have recently found a remarkable systematics in light flavor (u, d and s) baryons [6, 7]. The systematics applies essentially to all SU(3) baryons including almost 80 % of the observed states nominated by the Particle Data Group [8, 9]. The resulting common structure of baryon spectra then look very much like a rotational band. This in turn implies that excited baryons are likely to be deformed in space. In fact, the idea of deformed baryons is not new [10, 11]. However, our finding has shown that the picture holds for more baryons than it was originally thought. Furthermore, it turns out that a very simple non-relativistic quark model with a deformed oscillator potential can explain this aspect at once. This is indeed a remarkable fact since the model essentially contains only one parameter. We call the model the deformed oscillator quark (DOQ) model as described in detail in Refs. [6, 7]

Naturally as a next step, an interesting question arises; how does the DOQ model describe various transition processes? This is the issue we would like to address in this paper. For this we study the electromagnetic transitions of excited baryons. In principle, we can consider various transitions between both excited and ground states. Experimentally, however, only transitions from the ground state nucleon to excited states are observed, where experimental amplitudes are compiled in the form of the helicity amplitudes $A_{1/2}$ and $A_{3/2}$ [9, 12, 13, 14].

We compute transition amplitudes first in the multipole basis in analogy with nuclear transitions. One significant difference, however, between the baryon and nuclear transitions is that in the latter the long wave length approximation can be used as the typical energy scale is a few

MeV, while in the baryonic case, the same approximation can not be used since the relevant transition energy is compatible with the inverse length of a typical baryon size.

The plan of this paper is as follows. In section 2, we introduce the DOQ model and briefly discuss the mass spectrum of SU(3) baryons [6, 7]. Then we present wave functions for the deformed excited states which are necessary for the computation of transition amplitudes. In section 3, we study electromagnetic transitions and derive various matrix elements. We discuss carefully theoretical amplitudes that can be compared with empirical amplitudes including their signs. Appropriate treatment of the sign requires additional information of the pion coupling, which we also discuss. In section 4, we compare theoretical amplitudes with experimental data. After discussing the results in the naive DOQ model, we consider two important effects which are missing in our previous study. They are diagonalization of the non-orthogonal basis and relativistic effects. We pay special attention to the transition of the Roper resonance, since this is the channel for which theoretical explanation is difficult. Final section 5 is devoted to the summary of the present work.

2 Deformed Oscillator Quark Model

In this section we briefly discuss the DOQ model for excited baryons [11, 15], and present necessary ingredients to compute transition amplitudes.

2.1 Deformed intrinsic states and rotational spectra

Let us start with the Hamiltonian of the DOQ model:

$$H^{\text{DOQ}} = \sum_{i=1}^3 \left(\frac{\vec{p}_i^2}{2m} + \frac{m}{2} (\omega_x^2 x_i^2 + \omega_y^2 y_i^2 + \omega_z^2 z_i^2) \right). \quad (2-1)$$

Here the index i runs over three valence quarks. The masses of constituent quarks m is taken about 300 MeV for u , d and s quarks. Practically, in the harmonic oscillator model, only relevant parameters are the oscillator parameters ω_i and the actual value of m is not important.

Applying the following coordinate transformation

$$\begin{aligned} \vec{R} &= \frac{1}{\sqrt{3}}(\vec{x}_1 + \vec{x}_2 + \vec{x}_3), \\ \vec{\rho} &= \frac{1}{\sqrt{2}}(\vec{x}_1 - \vec{x}_2), \\ \vec{\lambda} &= \frac{1}{\sqrt{6}}(\vec{x}_1 + \vec{x}_2 - 2\vec{x}_3), \end{aligned} \quad (2-2)$$

the center of mass coordinate can be removed and the resulting intrinsic hamiltonian is given as

$$H^{\text{int}} = \frac{\vec{p}_\rho^2}{2m} + \frac{m}{2} (\omega_x^2 \rho_x^2 + \omega_y^2 \rho_y^2 + \omega_z^2 \rho_z^2) + (\rho \rightarrow \lambda). \quad (2-3)$$

The eigenstates of the intrinsic hamiltonian (2-3) are specified by a set of oscillator quantum numbers $(n_x^\rho, n_y^\rho, n_z^\rho; n_x^\lambda, n_y^\lambda, n_z^\lambda)$ and the corresponding eigenenergies are given by

$$\begin{aligned} E^{\text{int}} &= (n_x^\rho + \frac{1}{2})\omega_x + (n_y^\rho + \frac{1}{2})\omega_y + (n_z^\rho + \frac{1}{2})\omega_z + (\rho \rightarrow \lambda) \\ &= (N_x + 1)\omega_x + (N_y + 1)\omega_y + (N_z + 1)\omega_z, \end{aligned} \quad (2-4)$$

where $N_x = n_x^\rho + n_x^\lambda$, $N_y = n_y^\rho + n_y^\lambda$, $N_z = n_z^\rho + n_z^\lambda$. Thus the intrinsic energy (2-4) is regarded as a function of N_x , N_y , N_z and ω 's.

For a given (N_x, N_y, N_z) , the energy minimization is performed with respect to the deformation $\delta\omega_x$, $\delta\omega_y$ and $\delta\omega_z$. Unless we have some additional conditions, the variation leads to the trivial result; $E^{\text{int}} \rightarrow 0$, when $\omega_x = \omega_y = \omega_z \rightarrow 0$. In order to avoid this collapse of the system, we impose the volume conservation condition $\omega_x\omega_y\omega_z = \omega^3 = \text{const}$. The validity of such an assumption depends on the underlying dynamics of quark confinement. In fact, one may relax the volume conservation by, for example, adding a term like $B/(\omega_x\omega_y\omega_z)^p$ to the energy (2-4). It turns out, however, that the result does not change very much, and therefore we simply adopt the condition of volume conservation.

Now the minimum energy of (2-4) is given by

$$E^{\text{int}} = 3(N_x + 1)^{1/3}(N_y + 1)^{1/3}(N_z + 1)^{1/3}\omega, \quad (2-5)$$

when

$$\omega_x : \omega_y : \omega_z = \frac{1}{N_x + 1} : \frac{1}{N_y + 1} : \frac{1}{N_z + 1}. \quad (2-6)$$

The inverse relation of (2-6) is slightly convenient as it gives the ratio of the lengths of axes of the deformed state:

$$a_x : a_y : a_z = N_x + 1 : N_y + 1 : N_z + 1, \quad (2-7)$$

where $a_{x,y,z}$ are root mean square lengths of the x, y, z directions. The ground state with $N = 0$ ($N_x = N_y = N_z = 0$) yields the spherically symmetric intrinsic state just as in the conventional quark model. For excited states $N = 1$ ($N_x = N_y = 0, N_z = 1$ when the z -axis is chosen as a symmetry axis), the intrinsic state deforms prolately with the ratio of short to long axes $1 : 2$. The energy of this deformed state is 3.780ω as compared to 4ω of the spherical quark model. For excited states $N = 2$, there are two cases. One is $N_x = N_y = 0, N_z = 2$ for the prolate deformation with the ratio of short to long axes $1 : 3$. The energy is 4.327ω as compared to 5ω of the spherical state with $(n, l) = (0, 2)$ or $(1, 0)$. Another is $N_x = N_y = 1, N_z = 0$ which yields the oblate deformation with the ratio of short to long axes $1 : 2$, whose energy is 4.762ω . In general, the prolate shape takes the minimum energy for a given $N = N_x + N_y + N_z$, and so, in the following discussions we consider only the prolate deformation with the symmetry axis chosen along the z direction. We summarize in Table 1 physical quantities of prolately deformed states.

Since the deformed states break rotational symmetry, it should be recovered for eigenstates of angular momentum l . This can be performed by the standard cranking method [15]. The key quantities are the moment of inertia \mathcal{I} and the angular momentum fluctuation $\langle l^2 \rangle$ of the

Table 1: Various quantities of prolately deformed states. Dimensional quantities are scaled by an appropriate power of ω .

Positive parity						Negative parity					
N	d	E^{int}	$E^{\text{spherical}}$	$1/2\mathcal{I}$	$\langle l^2 \rangle$	N	d	E^{int}	$E^{\text{spherical}}$	$1/2\mathcal{I}$	$\langle l^2 \rangle$
0	1	—	3	—	0						
2	3	4.33	5	0.0721	8	1	2	3.78	4	0.126	3
4	5	5.13	7	0.0329	24	3	4	4.76	6	0.0467	15
6	7	5.74	9	0.0191	48	5	6	5.45	8	0.0246	35

Table 2: Excitation energies of the $N = 2$ and $N = 1$ rotational bands. Energy values in units of MeV are computed by using $\omega = 644$ MeV. [7]

$N = 2$			$N = 1$		
l	$E(N = 2, l) - E(N = 0)$		l	$E(N = 1, l) - E(N = 0)$	
	in ω	in MeV		in ω	in MeV
0	0.750	483	1	0.654	421
2	1.183	752	3	1.914	1230
4	2.192	1410	5	4.182	2690

deformed state. In the DOQ model, they can be computed analytically. For a prolately deformed state of z -axis symmetry ($\omega_x = \omega_y \neq \omega_z$), they are given by

$$\mathcal{I}_N = \left(\frac{N_z + 1}{\omega_z} + \frac{N_y + 1}{\omega_y} \right) = \frac{1}{(N+1)^{1/3}} (N^2 + 2N + 2) \frac{1}{\omega}, \quad (2-8)$$

$$\langle l^2 \rangle_N = \left(\left(\frac{\omega_x}{\omega_z} \right)^2 - 1 \right) = N(N+2), \quad (2-9)$$

The rotational band is then constructed for each N :

$$E_{Nl} = E_N^{\text{int}} - \frac{1}{2\mathcal{I}_N} \langle l^2 \rangle_N + \frac{1}{2\mathcal{I}_N} l(l+1). \quad (2-10)$$

Numerical values for \mathcal{I} and $\langle l^2 \rangle$ are shown in Table 1, and the rotational energies E_{Nl} for the $N = 2$ and $N = 1$ bands are shown in Table 2. We emphasize that the energy subtraction due to angular momentum fluctuation, the second term of (2-10), is very important to make the theoretical masses down close to experimental values. This is particularly important for the first $1/2^+$ excited state (the Roper).

Coupling the intrinsic spin s of three quarks with the orbital angular momentum l , take for example $s = 1/2$, we consider mass spectra of the $N = 2$ and $N = 1$ bands for nucleon excited states as shown in Fig. 1. On the left hand side we show the theoretical results: one for the positive parity states of $l = 0, 2, 4, \dots$ and the other for the negative parity states of $l = 1, 3, \dots$. In the theoretical side, two spin states $j = l \pm 1/2$ degenerate when spin-orbit coupling is ignored, as experimental data suggest. On the right hand side, experimental masses of well observed nucleon excited states with four stars are shown [8]. One exception is the $5/2^-$ state of $D_{15}(2200)$ with two stars. This state is very likely to form a spin doublet with $G_{17}(2190)$. We do not list all the states but those which are well identified with the 28 representations ($s = 1/2$) of the spin-flavor group, and are well compared with the DOQ model predictions. Our theoretical formula for a fixed N ($N = 2$ for positive and $N = 1$ for negative parity states) corresponds to the rigid rotor approximation. Theoretically, one may consider effects from higher rotational bands of $N \geq 3$ in order to account for the softness of the intrinsic state. This is discussed in Ref. [16].

The mass formula (2-10) should be compared with excitation energies of baryons. Hence it contains essentially one parameter, which is the oscillator parameter ω . It is determined here by the average mass splitting between the first excited states of $1/2^+$ (Roper like states) and the corresponding ground states for the flavor SU(3) baryons (for details of SU(3) baryons, see the discussion below). The resulting value is $\omega = 644$ MeV [7]. Considering the simplicity of the DOQ model, it is remarkable that many observed states fit very well to the theoretical rotational band. In particular we note that the first $1/2^+$ excited state of the Roper resonance emerges as the band head of the $N = 2$ rotational band.

If the fundamental structure of the excitation spectrum is produced by gluon dynamics of quark confinement, we should see a similar pattern in other members of the spin and flavor multiplets. In a recent publication, we have analyzed in detail the mass spectrum of SU(3) baryons and found that the picture of deformed baryons works extremely well for a wide class of baryons [6, 7]. We have been able to explain almost 80 % of the observed baryons as they fit into the rotational bands of the DOQ model.

Figure 1: Experimental nucleon mass spectra as compared with the DOQ predictions.

2.2 Three quark states

Baryon wave functions consist of spatial, spin, isospin and color parts. Here we discuss mainly spatial wave functions with definite permutation symmetry and with a good angular momentum. Since detailed method is found in Ref. [11], we summarize minimally what we need in the computation of transition amplitudes.

First we consider single particle wave functions in the deformed oscillator potential. They are given as products of one-dimensional harmonic oscillator wave functions $\psi_n(\vec{x})$:

$$\psi_{n_x n_y n_z}(\vec{x}) = \psi_{n_x}(x) \psi_{n_y}(y) \psi_{n_z}(z) . \quad (2-11)$$

Since we are interested in excited states of prolate shape, we set $n_x = n_y = 0$, and write (2-11) as $\psi_{00\nu}(\vec{x}) = \psi_0(x) \psi_0(y) \psi_\nu(z)$.

The state with a definite permutation symmetry for a three quark system, after removing the center of mass coordinates, is given by the product of the single particle wave functions $\psi_{00n}(\vec{\rho})$ and $\psi_{00n'}(\vec{\lambda})$ with the constraint $n + n' = N$. They are either totally symmetric (S) or mixed symmetric (MS)⁴. The MS states are further classified into two types of ρ and λ symmetries. Here we summarize single particle wave functions and the resulting intrinsic states for deformed baryons, $\Psi^{N\sigma}(\vec{\rho}, \vec{\lambda})$, where σ represents a permutation symmetry (S , λ or ρ). In the following we introduce the parameter $\alpha = \sqrt{m\omega}$ and the deformation parameter $d = \omega_x/\omega_z$. As we see in the previous section, d becomes $N + 1$ after the energy minimization. However, we keep it in the following expressions of wave functions to compute transition amplitudes as functions of the deformation parameter d .

⁴For the prolate deformation, there is no totally antisymmetric wave function like $\Psi^{NA} = \phi_{100}(\rho)\phi_{001}(\lambda) - \phi_{001}(\rho)\phi_{100}(\lambda)$, since quarks excite along only one direction, where $(n_x = n_y = 0, n_z \neq 0)$.

- Single particle wave function

$$\begin{aligned}
\psi_{000}(\vec{x}) &= \left(\frac{\alpha^2}{\pi}\right)^{\frac{3}{4}} \exp(-\frac{\alpha^2}{2}\{d^{\frac{1}{3}}(x^2 + y^2) + d^{-\frac{2}{3}}z^2\}) \\
\psi_{001}(\vec{x}) &= \left(\frac{\alpha^2}{\pi}\right)^{\frac{3}{4}} \sqrt{2}d^{-\frac{1}{3}}\alpha z \exp(-\frac{\alpha^2}{2}\{d^{\frac{1}{3}}(x^2 + y^2) + d^{-\frac{2}{3}}z^2\}) \\
\psi_{002}(\vec{x}) &= \left(\frac{\alpha^2}{\pi}\right)^{\frac{3}{4}} \sqrt{2}(d^{-\frac{2}{3}}\alpha^2 z^2 - \frac{1}{2}) \exp(-\frac{\alpha^2}{2}\{d^{\frac{1}{3}}(x^2 + y^2) + d^{-\frac{2}{3}}z^2\})
\end{aligned} \tag{2-12}$$

- Three quark state

- * $N = 0$ (Spherical ground state) : $d = 1$

$$\Psi^{0S}(\vec{\rho}, \vec{\lambda}) = \psi_{000}(\vec{\rho})\psi_{000}(\vec{\lambda}) \tag{2-13}$$

- * $N = 1$ (Negative parity excitations) : $d = 2$

$$\begin{aligned}
\Psi^{1\rho}(\vec{\rho}, \vec{\lambda}) &= \psi_{001}(\vec{\rho})\psi_{000}(\vec{\lambda}) \\
\Psi^{1\lambda}(\vec{\rho}, \vec{\lambda}) &= \psi_{000}(\vec{\rho})\psi_{001}(\vec{\lambda})
\end{aligned} \tag{2-14}$$

- * $N = 2$ (Positive parity excitations) : $d = 3$

$$\begin{aligned}
\Psi^{2S}(\vec{\rho}, \vec{\lambda}) &= \frac{1}{\sqrt{2}} \left(\psi_{002}(\vec{\rho})\psi_{000}(\vec{\lambda}) + \psi_{000}(\vec{\rho})\psi_{002}(\vec{\lambda}) \right) \\
\Psi^{2\rho}(\vec{\rho}, \vec{\lambda}) &= \psi_{001}(\vec{\rho})\psi_{001}(\vec{\lambda}) \\
\Psi^{2\lambda}(\vec{\rho}, \vec{\lambda}) &= \frac{1}{\sqrt{2}} \left(\psi_{002}(\vec{\rho})\psi_{000}(\vec{\lambda}) - \psi_{000}(\vec{\rho})\psi_{002}(\vec{\lambda}) \right)
\end{aligned} \tag{2-15}$$

Since these deformed intrinsic states (2-14) and (2-15) are not eigenstates of angular momentum, we need to project out the states with good angular momentum for physical baryons. The projection method is conveniently performed first by expanding the deformed single particle state $\psi_{00\nu}(\vec{x})$ by the wave functions $\phi_{nl,m=0}$ of the spherical three dimensional harmonic oscillator:

$$\psi_{00\nu}(\vec{x}) = \sum_{nl} C_{nl}^{\nu} \phi_{nl,m=0} \equiv \sum_{nl} C_{nl}^{\nu} \phi_{nl} . \tag{2-16}$$

The constraint $m = 0$ reflects the axial symmetry around the z -axis. Substituting (2-16) in Eqs. (2-14) and (2-15), we find for three quark states Ψ :

$$\Psi^{N\sigma}(\vec{\rho}, \vec{\lambda}) = \sum_{n_{\rho}l_{\rho}n_{\lambda}l_{\lambda}} F_{n_{\rho}l_{\rho}n_{\lambda}l_{\lambda}}^{N\sigma} \phi_{n_{\rho}l_{\rho}}(\vec{\rho})\phi_{n_{\lambda}l_{\lambda}}(\vec{\lambda}) , \tag{2-17}$$

where the coefficients $F_{n_{\rho}l_{\rho}n_{\lambda}l_{\lambda}}^{N\sigma}$ are given by

$$\begin{aligned}
F_{n_{\rho}l_{\rho}n_{\lambda}l_{\lambda}}^{1\rho} &= C_{n_{\rho}l_{\rho}}^1 C_{n_{\lambda}l_{\lambda}}^0 , \\
F_{n_{\rho}l_{\rho}n_{\lambda}l_{\lambda}}^{1\lambda} &= C_{n_{\rho}l_{\rho}}^0 C_{n_{\lambda}l_{\lambda}}^1 , \\
F_{n_{\rho}l_{\rho}n_{\lambda}l_{\lambda}}^{2S} &= \frac{1}{\sqrt{2}} \left(C_{n_{\rho}l_{\rho}}^2 C_{n_{\lambda}l_{\lambda}}^0 + C_{n_{\rho}l_{\rho}}^0 C_{n_{\lambda}l_{\lambda}}^2 \right) , \\
F_{n_{\rho}l_{\rho}n_{\lambda}l_{\lambda}}^{2\rho} &= C_{n_{\rho}l_{\rho}}^1 C_{n_{\lambda}l_{\lambda}}^1 , \\
F_{n_{\rho}l_{\rho}n_{\lambda}l_{\lambda}}^{2\lambda} &= \frac{1}{\sqrt{2}} \left(C_{n_{\rho}l_{\rho}}^2 C_{n_{\lambda}l_{\lambda}}^0 - C_{n_{\rho}l_{\rho}}^0 C_{n_{\lambda}l_{\lambda}}^2 \right) .
\end{aligned} \tag{2-18}$$

The states with definite angular momentum l, m can readily be projected out by operating the projection operator [17, 18],

$$\hat{P}_{lm} = \int d[A] D_{m0}^{l*}(A) \mathcal{R}_\rho(A) \mathcal{R}_\lambda(A), \quad (2-19)$$

where $\mathcal{R}_\rho(A)$ and $\mathcal{R}_\lambda(A)$ are the rotation operator acting on the ρ and λ variables, and A denotes a set of Euler angles for rotation. Applying \hat{P}_{lm} to the deformed intrinsic state (2-17), we find

$$\Psi_{lm}^{N\sigma} \equiv \hat{P}_{lm} \Psi^{N\sigma} = \mathcal{N} \sum_{n_\rho l_\rho n_\lambda l_\lambda} F_{n_\rho l_\rho n_\lambda l_\lambda}^{N\sigma} (l_\rho \ 0 \ l_\lambda \ 0 | l \ 0) [\phi_{n_\rho l_\rho} \times \phi_{n_\lambda l_\lambda}]^{lm}, \quad (2-20)$$

where $[\phi_{n_\rho l_\rho} \times \phi_{n_\lambda l_\lambda}]^{lm}$ expresses that $\phi_{n_\rho l_\rho}$ and $\phi_{n_\lambda l_\lambda}$ are coupled to the state with total angular momentum (l, m) , and $(l_\rho \ 0 \ l_\lambda \ 0 | l \ 0)$ are the standard Clebsh-Gordan coefficients. The normalization constants \mathcal{N} in (2-20) are given by

$$\mathcal{N}^{-2} = \sum_{n_\rho l_\rho n_\lambda l_\lambda} |F_{n_\rho l_\rho n_\lambda l_\lambda}^{N\sigma} (l_\rho \ 0 \ l_\lambda \ 0 | l \ 0)|^2. \quad (2-21)$$

Here we have performed angular momentum projection after taking variation (PAV) with respect to ω 's. One could get better wave function through angular momentum projection before variation (PBV). We have checked the PBV and found that the difference between the two projection schemes is not very significant up to $l = 2$.

Finally to close this section, we write spatial-spin-flavor wave functions which are totally symmetric. Let us denote spin and isospin wave functions by χ and ϕ , respectively, with a superscript ρ, λ or S . For nucleon states (denoted by N) with isospin 1/2, there are three possible states for a given spin and parity j^P ($P = (-1)^l$):

$$\begin{aligned} \text{(N1)} \quad |N; [l_S, 1/2]^j\rangle &= \frac{1}{\sqrt{2}} \left([\Psi_l^{NS}, \chi^\rho]^j \phi^\rho + [\Psi_l^{NS}, \chi^\lambda]^j \phi^\lambda \right), \\ \text{(N2)} \quad |N; [l_{MS}, 1/2]^j\rangle &= \frac{1}{2} \left([\Psi_l^{N\rho}, \chi^\rho]^j \phi^\lambda + [\Psi_l^{N\rho}, \chi^\lambda]^j \phi^\rho \right. \\ &\quad \left. + [\Psi_l^{N\lambda}, \chi^\rho]^j \phi^\rho - [\Psi_l^{N\lambda}, \chi^\lambda]^j \phi^\lambda \right), \\ \text{(N3)} \quad |N; [l_{MS}, 3/2]^j\rangle &= \frac{1}{\sqrt{2}} \left([\Psi_l^{N\rho}, \chi^S]^j \phi^\rho + [\Psi_l^{N\lambda}, \chi^S]^j \phi^\lambda \right). \end{aligned} \quad (2-22)$$

On the left hand side, the notation is such that the orbital wave function is labeled simply by the angular momentum l and permutation symmetry σ, l_σ . The orbital angular momentum is then coupled with the three quark spin $s = 1/2$ or $3/2$ to yield the total nucleon spin j . For deltas with isospin 3/2, there are two possible states for a given j^P :

$$\begin{aligned} \text{(\Delta1)} \quad |\Delta; [l_S, 3/2]^j\rangle &= [\Psi_l^{NS}, \chi^S]^j \phi^S, \\ \text{(\Delta2)} \quad |\Delta; [l_{MS}, 1/2]^j\rangle &= \frac{1}{\sqrt{2}} \left([\Psi_l^{N\rho}, \chi^\rho]^j + [\Psi_l^{N\lambda}, \chi^\lambda]^j \right) \phi^S. \end{aligned} \quad (2-23)$$

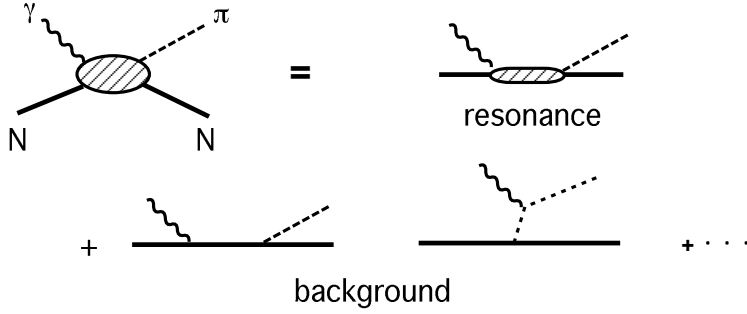


Figure 2: Pion photoproduction which is decomposed into resonance and background terms.

3 Electromagnetic Transitions

3.1 Helicity amplitudes for the pion photoproduction

Experimentally, electromagnetic couplings of excited baryon are extracted from single pion photoproductions (Fig. 2). In a resonance dominant model, production amplitudes are assumed to be decomposed into the Born terms and resonance contributions. A distinguished feature of this process is that not only the magnitude but also the sign of the resonance contributions can be determined relative to the sign of the Born terms [12, 13, 14]. More precisely, the sign ϵ in the following combination can be determined experimentally:

$$\langle N | H_\pi | N^* \rangle \cdot \langle N^* | H_\gamma | N \rangle \equiv \epsilon |\langle N | H_\pi | N^* \rangle \cdot \langle N^* | H_\gamma | N \rangle|, \quad (3-1)$$

where H_π and H_γ are the interaction Hamiltonian for the pion and photon couplings. The sign ϵ is then included in the electromagnetic couplings $\langle N^* | H_\gamma | N \rangle$. Therefore, in theoretical calculations, both the electromagnetic and pion couplings have to be calculated simultaneously. Ignorance of the pion coupling part might lead to incorrect results for the sign.

Usually experimental amplitudes (T -matrix) are presented in the helicity basis, which are given as matrices in the space spanned by the initial and final helicity states [12, 13]. They are also functions of the scattering angles θ and ϕ . The helicity amplitudes are then expanded by multipoles as [19]

$$A_{\mu\lambda}(\theta, \phi) = \sum_j (2j+1) A_{\mu\lambda}^j d_{\lambda\mu}^j(\theta) e^{i(\lambda-\mu)\phi}. \quad (3-2)$$

Here $\lambda = \lambda_\gamma - \lambda_i$ and $\mu = \lambda_\pi - \lambda_f = -\lambda_f$ are the initial and final state helicities with λ_γ , λ_i , λ_π and λ_f being the helicity of the photon, of the initial nucleon, of the pion and of the final nucleon, respectively. In the pion photoproduction, λ takes four values of $-3/2, -1/2, +1/2$ and $+3/2$, while $\mu = -1/2$ and $+1/2$. Among the eight components of $A_{\mu\lambda}$, four of them are independent due to time reversal symmetry. The expansion coefficients $A_{\mu\lambda}^j$ which were called the helicity elements in the literature [12] contain dynamical information of the excited states

of the total spin j . The helicity elements $A_{\mu\lambda}^j$ in its form, however, do not have a definite parity. Parity eigenstates are projected out by the following linear combinations [12, 13, 19]:

$$C_{\lambda}^{l_{\pi}+} = \frac{1}{\sqrt{2}} \left(A_{1/2\lambda}^j + A_{-1/2\lambda}^j \right), \quad (3-3)$$

$$C_{\lambda}^{(l_{\pi}+1)-} = \frac{1}{\sqrt{2}} \left(A_{1/2\lambda}^j - A_{-1/2\lambda}^j \right), \quad (3-4)$$

where the total spin j is given by $j = l_{\pi} + 1/2$, and the parity is $P = -(-)^{l_{\pi}}$ for $C_{\lambda}^{l_{\pi}+}$ and $P = (-)^{l_{\pi}}$ for $C_{\lambda}^{(l_{\pi}+1)-}$. Here l_{π} is the orbital angular momentum of the pion in the final state.

Resonance parameters are determined by fitting the experimental amplitudes (3-3) and (3-4) by a simple Breit-Wigner form assuming resonance dominance [20]⁵:

$$\begin{aligned} C_{\lambda}^{l_{\pi}\pm}(W) &= -\sum_{N^*} \epsilon \left(\frac{\Gamma_{\gamma}^{\lambda} \Gamma_{\pi}}{kq} \right)^{1/2} \frac{M}{W^2 - M^{*2} - iM\Gamma} + \text{background} \\ &\rightarrow i \epsilon \left(\frac{\Gamma_{\gamma}^{\lambda} \Gamma_{\pi}}{kq\Gamma^2} \right)^{1/2}, \end{aligned} \quad (3-5)$$

where Γ is the total decay width of the resonance N^* , $\Gamma_{\gamma}^{\lambda}$ and Γ_{π} are the partial width for gamma (with the helicity λ) and pion emission. k and q are the momentum carried by the photon and the pion, respectively. In the second line of (3-5) the CM energy W is set to the resonance energy M^* , where the single resonance N^* is assumed to dominate the amplitude. The relative sign of each term is included in the parameter $\epsilon = \pm 1$. The helicity amplitudes for the electromagnetic couplings A_{λ}^{jP} are then defined by the imaginary part of the amplitude:

$$A_{\lambda}^{jP} = -i \left(\frac{1}{(2j+1)\pi} \frac{k}{q} \frac{M}{M^*} \frac{\Gamma_{\pi}}{\Gamma^2} \right)^{-1/2} C_{\lambda}^{l_{\pi}\pm}(M^*) C_{\pi N}, \quad j = l_{\pi} \pm 1/2, \quad P = -(-)^{l_{\pi}}, \quad (3-6)$$

where $C_{\pi N}$ is the isospin Clebsh-Gordan coefficient for the decay of N^* into the relevant πN charge state [9]. In this equation, the strength of the pion coupling in $C_{\lambda}^{l_{\pi}\pm}$ is removed by multiplying the factor $\Gamma_{\pi}^{-1/2}$.

Theoretically, the amplitude $C_{\lambda}^{l_{\pi}\pm}(M^*)$ may be computed as

$$\begin{aligned} C(W) &= i \langle N | H_{\pi} | N^* \rangle \frac{M}{W^2 - M^{*2} - iM\Gamma} \langle N^* | H_{\gamma} | N \rangle \\ &\xrightarrow{W \rightarrow M^*} \langle N | H_{\pi} | N^* \rangle \langle N^* | H_{\gamma} | N \rangle \frac{1}{\Gamma}. \end{aligned} \quad (3-7)$$

From this and (3-6), one obtains an alternative expression

$$A_{\lambda} = -\epsilon (KF) (-i)^l \langle N^* | H_{\gamma} | N \rangle, \quad (KF) = \sqrt{\frac{E_N(k)}{2\omega M}}, \quad (3-8)$$

where l is an orbital angular momentum of an excited quark in N^* , and ϵ is the sign extracted from, together with another phase factor $(-i)^l$, the pion matrix element as given in Appendix B. At the end of this subsection, we summarize selection rules for various amplitudes and excited states in Table 3.

⁵Note that the expression the resonance propagator (3-5) differs from that given in Refs. [13, 14]. However, (3-5) agrees with, for instance, eq. (2-18) of Ref. [13].

Table 3: Relation between various amplitudes and quark model states.

Excited states		Photon couplings		Pion photoproduction		
j^P	$[l, s]^j$	Multipole	Helicity	l_π	Multipole	Helicity
$1/2^+$	$[0, 1/2]^{1/2}$	$M1$	$A_{1/2}$	1	M_{1-}	$C_{1/2}^{1-}$
	$[2, 3/2]^{1/2}$					
$3/2^+$	$[2, 1/2]^{3/2}$	$M1, E2$	$A_{1/2, 3/2}$	1	M_{1+}, E_{1+}	$C_{1/2, 3/2}^{1+}$
	$[0, 3/2]^{3/2}$	$M1$				
$5/2^+$	$[2, 1/2]^{5/2}$	$M3, E2$	$A_{1/2, 3/2}$	3	M_{3-}, E_{3-}	$C_{1/2, 3/2}^{3-}$
	$[4, 3/2]^{3/2}$	$M3$				
$1/2^-$	$[1, 1/2]^{1/2}$	$E1$	$A_{1/2}$	0	E_{0+}	$C_{1/2}^{0+}$
	$[1, 3/2]^{1/2}$					
$3/2^-$	$[1, 1/2]^{3/2}$	$M2, E1$	$A_{1/2, 3/2}$	2	M_{2-}, E_{2-}	$C_{1/2, 3/2}^{2-}$
	$[3, 3/2]^{3/2}$	$M2$				
$5/2^-$	$[3, 1/2]^{5/2}$	$M2, E3$	$A_{1/2, 3/2}$	2	M_{2+}, E_{2+}	$C_{1/2, 3/2}^{2+}$
	$[1, 3/2]^{3/2}$	$M2$				

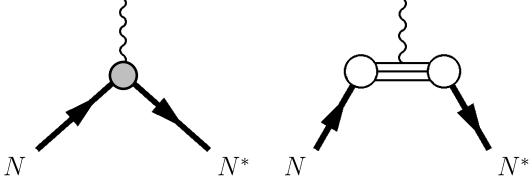


Figure 3: A photon coupling to a quark in baryons.

3.2 Photon couplings

The electromagnetic coupling is given by the interaction hamiltonian

$$H_\gamma = -e \int d^3x \vec{J} \cdot \vec{A}, \quad (3-9)$$

where \vec{A} is the photon field, and for the current \vec{J} we adopt the non-relativistic form

$$\begin{aligned} \vec{J} &= \sum_{j=1}^3 \vec{J}^{(j)} = 3\vec{J}^{(3)}, \\ \vec{J}^{(3)} &= \frac{1}{2m} \left(u_f^\dagger (i \vec{\nabla} - i \vec{\nabla}) u_i + \vec{\nabla} \times (u_f^\dagger \vec{\sigma} u_i) \right) \tau_\mu. \end{aligned} \quad (3-10)$$

Here we have used overall permutation symmetry of quarks in the baryons, and u_i and u_f are the two component Pauli spinors for the initial and final state quarks, respectively (see Fig. 3). The isospin matrix τ_μ is either $\tau_0 = 1$ for the isoscalar current and $\tau_i = \tau_3$ for the isovector current. We will consider relativistic corrections later.

Helicity amplitudes $A_{1/2, 3/2}$ are then computed as given in (3-8):

$$\begin{aligned} A_{1/2} &= -\epsilon(-i)^l (KF) \langle N^*(j, 1/2) | \vec{J} \cdot \vec{A}_{+1} | N(1/2, -1/2) \rangle, \\ A_{3/2} &= -\epsilon(-i)^l (KF) \langle N^*(j, 3/2) | \vec{J} \cdot \vec{A}_{+1} | N(1/2, 1/2) \rangle. \end{aligned} \quad (3-11)$$

In order to relate the helicity amplitudes with the multipole amplitudes, we consider the multipole expansion for the photon field ⁶

$$\vec{A}_\lambda = \vec{\epsilon}_\lambda e^{i\vec{k}\cdot\vec{x}}. \quad (3-12)$$

Here $\vec{\epsilon}_\lambda$ is the polarization vector of helicity $\lambda = \pm 1$. The momentum \vec{k} is related to the physical momentum \vec{k}_{phys} by

$$\vec{k} = \sqrt{\frac{2}{3}} \vec{k}_{phys}, \quad (3-13)$$

in the convention of coordinate transformation (2-2). If we choose the z-axis along the direction of photon propagation \vec{k} , the plane wave of a definite helicity (3-12) can be expanded by multipoles as [21]

$$\vec{A}_\lambda = -\sqrt{2\pi} \sum_{l=1}^{\infty} i^l \sqrt{2l+1} \left(\lambda \vec{A}_{l\lambda}^{(M)} + i \vec{A}_{l\lambda}^{(E)} \right). \quad (3-14)$$

Here the magnetic (M) and electric (E) multipole fields are given by

$$\begin{aligned} \vec{A}_{lm}^{(M)}(\vec{r}) &= j_l(kr) \vec{Y}_{lm}^l(\hat{r}), \quad \vec{Y}_{lm}^l = \frac{1}{\sqrt{l(l+1)}} \vec{L} Y_{lm}(\hat{r}), \\ \vec{A}_{lm}^{(E)}(\vec{r}) &= -\frac{i}{k} \vec{\nabla} \times \vec{A}_{lm}^{(M)}(\vec{r}), \end{aligned} \quad (3-15)$$

where we have adopted the standard convention for the spherical harmonics [22], and $j_l(kr)$ are the spherical Bessel functions.

Substituting (3-14) in (3-9) and applying the Wigner-Eckart theorem to each multipole amplitude, we find the following formulae relating the helicity and multipole amplitudes:

For $j = l + 3/2$:

$$\begin{aligned} A_{1/2} &= -\epsilon(KF) \sqrt{2\pi} \sqrt{\frac{l+1}{2l+4}} \mathcal{M}(Ml+1) \\ A_{3/2} &= -\epsilon(KF) \sqrt{2\pi} \sqrt{\frac{l+3}{2l+4}} \mathcal{M}(Ml+1) \end{aligned} \quad (3-16)$$

For $j = l + 1/2$:

$$\begin{aligned} A_{1/2} &= \epsilon(KF) \sqrt{2\pi} \left(+\sqrt{\frac{l+2}{2l+2}} \mathcal{M}(Ml+1) - \sqrt{\frac{l}{2l+2}} \mathcal{M}(El) \right) \\ A_{3/2} &= \epsilon(KF) \sqrt{2\pi} \left(-\sqrt{\frac{l}{2l+2}} \mathcal{M}(Ml+1) - \sqrt{\frac{l+2}{2l+2}} \mathcal{M}(El) \right) \end{aligned} \quad (3-17)$$

For $j = l - 1/2$:

$$\begin{aligned} A_{1/2} &= \epsilon(KF) \sqrt{2\pi} \left(+\sqrt{\frac{l-1}{2l}} \mathcal{M}(Ml-1) + \sqrt{\frac{l+1}{2l}} \mathcal{M}(El) \right) \\ A_{3/2} &= \epsilon(KF) \sqrt{2\pi} \left(+\sqrt{\frac{l+1}{2l}} \mathcal{M}(Ml-1) - \sqrt{\frac{l-1}{2l}} \mathcal{M}(El) \right) \end{aligned} \quad (3-18)$$

⁶ The same symbol A is used for the photon field and helicity amplitudes, and ϵ for the photon polarization vector and the sign of the amplitudes. Both notations are standard and there will be no confusion in the following discussions.

For $j = l - 3/2$:

$$\begin{aligned} A_{1/2} &= -\epsilon(KF) \sqrt{2\pi} \sqrt{\frac{l}{2l-2}} \mathcal{M}(Ml-1) \\ A_{3/2} &= +\epsilon(KF) \sqrt{2\pi} \sqrt{\frac{l-2}{2l-2}} \mathcal{M}(Ml-1) \end{aligned} \quad (3-19)$$

Writing $|N\rangle \rightarrow |i\rangle$ and $|N^*\rangle \rightarrow |f\rangle$, the reduced matrix elements are defined by

$$\begin{aligned} \mathcal{M}(Ml) &\equiv i \langle f || \vec{J} \cdot \vec{A}_l^{(M)} || i \rangle \cdot \langle f | \tau_\mu | i \rangle , \\ \mathcal{M}(El) &\equiv i \langle f || \vec{J} \cdot \vec{A}_l^{(E)} || i \rangle \cdot \langle f | \tau_\mu | i \rangle , \end{aligned} \quad (3-20)$$

where the isospin part is the ordinary matrix elements. In these equations, the phase i is introduced to make the matrix elements \mathcal{M} pure real. Furthermore, in Eqs. (3-16) – (3-19), the phase factor $(-i)^l$ in (3-11) is canceled by another factor i^l coming from the multipole expansion (3-14).

Let us briefly outline how to compute the multipole amplitudes (3-20). For illustration, we consider magnetic transitions Ml . Let us write the reduced matrix element as

$$\langle f || \vec{J} \cdot \vec{A}_l^{(M)} || i \rangle \rightarrow \frac{1}{2m} \left(i u_f^\dagger (\overleftarrow{\nabla} - \overrightarrow{\nabla}) u_i + \overrightarrow{\nabla} \times (u_f^\dagger \vec{\sigma} u_i) \right) \cdot \vec{A}_l^{(M)} , \quad (3-21)$$

where on the right hand side it is understood that the integral and sum are taken over configuration and spin spaces. The initial and final states are written as u_i and u_f in order to indicate the operation of derivatives. The isospin part can be treated separately in a trivial manner and is not shown here. Now in (3-21) integrating the left derivative ($\overleftarrow{\nabla}$) terms by parts and using the relation $\overrightarrow{\nabla} \cdot \vec{A} = 0$ and $\hat{x} \cdot \vec{A}^{(M)} = 0$ (the radial vector \hat{x} appears when the derivative hits the spherical initial state which is the ground state nucleon), one finds that the convection ($\overleftarrow{\nabla} - \overrightarrow{\nabla}$) term vanishes. Thus only the spin term survives:

$$\mathcal{M}(Ml) = \frac{i}{2m} u_f^\dagger \vec{\sigma} u_i \cdot \overrightarrow{\nabla} \times \vec{A}_l^{(M)} . \quad (3-22)$$

Using the relation between the magnetic and electric fields (3-15), one arrives at the expression

$$\begin{aligned} \mathcal{M}(Ml) &= \frac{i}{2m} \left[-\sqrt{\frac{l}{2l+1}} \langle f || [Y_{l+1}\sigma]^l j_{l+1} || i \rangle \right. \\ &\quad \left. + \sqrt{\frac{l+1}{2l+1}} \langle f || [Y_{l-1}\sigma]^l j_{l-1} || i \rangle \right] \langle f | \tau_\mu | i \rangle . \end{aligned} \quad (3-23)$$

For electric transitions El , again integrating by parts, one finds

$$\mathcal{M}(El) = \frac{1}{m} u_f^\dagger \overrightarrow{\nabla} u_i \cdot \vec{A}_l^{(E)} + \frac{k}{2m} u_f^\dagger \vec{\sigma} u_i \cdot \vec{A}_l^{(M)} . \quad (3-24)$$

Since the initial state is spherical, the first term can be written as

$$(u_f^\dagger \overrightarrow{\nabla} u_i) \cdot \vec{A}_l^{(E)} = u_f^\dagger u_i' \hat{x} \cdot \vec{A}_l^{(E)} . \quad (3-25)$$

Then using the following properties of the spherical harmonics,

$$\hat{x} \cdot \vec{A}_{lm}^{(E)} = \sqrt{l(l+1)} \frac{j_l(kr)}{kr} Y_{lm} , \quad (3-26)$$

for the first term and

$$\vec{\sigma} \cdot \vec{A}_{lm}^{(M)} = \vec{\sigma} \cdot \vec{Y}_{lm}^l j_l(kr) = [Y_l, \sigma]^{lm} j_l(kr) , \quad (3-27)$$

for the second term of (3-24), one arrives at the expression

$$\mathcal{M}(El) = -i \left[\frac{\sqrt{l(l+1)}}{m} \langle f || Y_l \frac{j_l(kr)}{kr} || i' \rangle + \frac{k}{2m} \langle f || [Y_l \sigma]^l j_l(kr) || i \rangle \right] \langle f | \tau_\mu | i \rangle , \quad (3-28)$$

where $|i'\rangle = \partial/\partial r |i\rangle$. Equations (3-23) and (3-28) are the general expressions for electromagnetic transitions $N\gamma \rightarrow N^*$. Concrete expressions for various matrix elements are given in Appendix C.

4 Results and discussions

We have computed the matrix elements as given in (C-13) – (C-22) for various excited baryon states of $N = 1$ (negative parity) and $N = 2$ (positive parity) bands⁷. Matrix elements are then investigated as functions of the deformation parameter d . Note that the actual d 's, when determined by the energy minimization, are $d = 2$ for $N = 1$ and $d = 3$ for $N = 2$ bands, respectively. We use the oscillator parameter as determined from the mass spectrum: $\omega = 644$ MeV. For the photon momentum k we use the values computed from the theoretical masses of excited states. The use of the experimental values do not change the essential features in the following discussions.

We have computed the amplitudes for all the DOQ model states which contain more states than experimentally observed. For a more realistic treatment, we should consider configuration mixings due to residual interactions. They could be induced by gluon and meson exchange interactions. For instance, a tensor force between quarks strongly mixes the two states of $^2P_{MS}$ and $^4P_{MS}$ for $1/2^-$ $N(1535)$ and $N(1650)$ [3, 23].

In Tables 4-5, we summarize helicity amplitudes for photon couplings to nucleon and delta excitations. The first column is for the present results with suitable deformation ($d = 3$ for positive parity states and $d = 2$ for negative parity states) and the second column is for the spherical limit ($d = 1$) which corresponds to the conventional non-relativistic (NR) quark model. These theoretical values are then compared to experimental data listed in the third column, where we indicate observed states which are naively identified with one of the DOQ model states.

As explained in the preceding subsection, we have computed both the photon and pion couplings simultaneously. Therefore, there is no ambiguity in relative signs of the photon couplings. In the nucleon channels $5/2^+ (^2D_S)$ and $3/2^- (^2P_{MS})$, however, the signs of the present result do not agree with those of, for instance, the pioneering work by Feynman, Kislinger and Ravndal [24]. However, if we included the sign as tabulated by Moorhouse and Parsons [25],

⁷ We do not discuss the transition $\Delta(1232) \rightarrow N$, since in the DOQ model they both appear spherical states and the transitions are the same as for the spherical quark model.

Table 4: Helicity amplitudes of nucleon excitations.

Positive parity			$A_{1/2}$			$A_{3/2}$			
			$d = 3$	$d = 1$	Exp.	$d = 3$	$d = 1$	Exp.	
$1/2^+$	$^2S'_S$	p	+115	+25	-68 ± 5	—	—	—	$P_{11}(1440)$
		n	-74	-16	$+39 \pm 15$	—	—	—	
	$^2S_{MS}$	p	+16	+17	$+5 \pm 16$	—	—	—	$P_{11}(1710)$
		n	-5	-6	-5 ± 23	—	—	—	
	$^4D_{MS}$	p	0	0		—	—	—	
		n	+3	+4	-5 ± 23	—	—	—	
$3/2^+$	2D_S	p	+70	+113	$+52 \pm 39$	-22	-36	-35 ± 24	$P_{13}(1720)$
		n	-21	-34	-2 ± 26	0	0	-43 ± 94	
	$^2D_{MS}$	p	+57	+80		-18	-25		
		n	-40	-56		+18	+25		
	$^4D_{MS}$	p	0	0		0	0		
		n	-6	-8.5		+11	+15		
	$^4S_{MS}$	p	0	0		0	0		
		n	-12	-14		-20	-23		
$5/2^+$	2D_S	p	+8	+12	-17 ± 10	-44	-71	$+127 \pm 12$	$F_{15}(1680)$
		n	-26	-42	$+31 \pm 13$	0	0	-30 ± 14	
	$^2D_{MS}$	p	+6	+9		-36	-50		
		n	+15	+21		+36	+50		
	$^4D_{MS}$	p	0	0		0	0		
		n	-4	-6		-17	-24		
Negative parity			$A_{1/2}$			$A_{3/2}$			
			$d = 2$	$d = 1$	Exp.	$d = 2$	$d = 1$	Exp.	
$1/2^-$	$^2P_{MS}$	p	+142	+154	74 ± 11	—	—	—	$S_{11}(1535)$
		n	-117	-126	-72 ± 25	—	—	—	
	$^4P_{MS}$	p	0	0	48 ± 16	—	—	—	$S_{11}(1650)$
		n	+13	+14	-17 ± 37	—	—	—	
$3/2^-$	$^2P_{MS}$	p	-18	-19	-23 ± 9	-127	-137	163 ± 8	$D_{13}(1520)$
		n	+55	+59	-64 ± 8	+127	+137	-141 ± 11	
	$^4P_{MS}$	p	0	0	-22 ± 13	0	0	0 ± 19	$D_{13}(1700)$
		n	-6	-6	0 ± 56	-30	-33	-2 ± 44	
$5/2^-$	$^4P_{MS}$	p	0	0	$+19 \pm 12$	0	0	$+19 \pm 12$	$D_{15}(1675)$
		n	-22	-28	-47 ± 23	-31	-39	-69 ± 19	

Table 5: Helicity amplitudes of delta excitations

Positive parity	$A^{1/2}$			$A^{3/2}$			
	$d = 3$	$d = 1$	Exp.	$d = 3$	$d = 1$	Exp.	
$1/2^+$ $^2S_{MS}$	+12	+14		–	–	–	$P_{31}(1910)$
4D_S	+11	+18	-12 ± 30	–	–	–	
$3/2^+$ $^2D_{MS}$	–9	–14		+11	+18		$P_{33}(1920)$
4D_S	–12	–24		+20	+41		
$^4S'_S$	–54	–37	-20 ± 29	–94	–65	$+1 \pm 22$	$P_{33}(1600)$
$5/2^+$ $^2D_{MS}$	+28	+46		+22	+36		$F_{35}(1905)$
4D_S	–8	–16	27 ± 13	–33	–65	-47 ± 19	
Negative parity	$A^{1/2}$			$A^{3/2}$			
	$d = 2$	$d = 1$	Exp.	$d = 2$	$d = 1$	Exp.	
$1/2^-$ $^2P_{MS}$	–35	–40	19 ± 16	–	–	–	$S_{31}(1620)$
$3/2^-$ $^2P_{MS}$	+69	78	116 ± 17	+69	+78	77 ± 28	$D_{33}(1700)$

and an additional phase factor $i^{l=2}$ for the D -wave component in the multipole expansion (3-14), the present results agree with the results of FKR. The convention of the sign has not been considered seriously even in recent publications. In the work of Koniuk and Isgur [4], their convention was taken to reproduce empirical one, which has been followed by several literatures [26, 27, 28]. This situation was partly discussed by Capstick in Ref. [29].

In many channels, the DOQ model ($d = 2$ or 3) reproduces experimental amplitudes reasonably well including both signs and absolute values nearly to the same extent that the NR quark model ($d = 1$) does. This means that the d dependence is not very strong, which is somewhat surprising, since excited states are rather strongly deformed as $d = 2$ and 3 . A possible reason could be that the number of the relevant degrees of freedom for baryons, which are valence quarks, is not very large. If we, however, look closely at the numbers, the positive parity baryons have slightly stronger d dependence than the negative parity baryons, as d is larger for the former. Typically, as it is seen in the channel $3/2^+ \ ^2D_S$, $A_{1/2}^{\text{proton}}(d = 1) = 113 \times 10^{-3} \text{ GeV}^{-1/2}$ and $A_{1/2}^{\text{proton}}(d = 3) = 70 \times 10^{-3} \text{ GeV}^{-1/2}$ as compared with the experimental value $A_{1/2}^{\text{proton}}(\text{exp}) = 52 \pm 39 \times 10^{-3} \text{ GeV}^{-1/2}$.

Theoretical predictions differ most significantly for the first $1/2^+$ excited state for the Roper resonance; not only the magnitude but also the sign do not agree with data. The relevant amplitude is $A_{1/2}$ or $M1$. Indeed the discrepancy in the sign is puzzling, if the $1/2^+$ excitation is simply considered as a radial excitation of the ground state nucleon. It does not matter whether it is a single particle or collective excitation. Due to an S-wave nature of the orbital motion, spin structure and hence the magnetic moment of the excited state should be the same as the ground state. Now we know that the magnetic moments of the nucleon, the delta [30] and the M1 transition of the delta [31] are reasonably well explained by the quark model. Therefore, one would naively expect that the magnetic transition of the $1/2^+$ excited state were explained

as well as these transition amplitudes in the above.

The discrepancy in the sign is known for a long time and various ideas to overcome the problem have been proposed. In Ref. [26], deformation effects was considered to be one candidate of such. However, their conclusion was based on the wrong sign of the amplitude. In fact, the deformation is to increase the amplitude but with the wrong sign remained. Since the problem in the Roper resonance is in itself an interesting question, we discuss two important effects in the next two subsections.

In the end of this subsection, we comment on the sign of the amplitudes for the $N(1440)$ and $\Delta(1600)$. The latter is interpreted as the Roper resonance of the delta. Let us look at the formulae for the nucleon (C-13) and the delta for $d = 1$ when the sum in the radial integral reduces just to a single term. We have

$$\begin{aligned} M1(N; {}^2S'_S) &= \frac{3}{4\sqrt{2}} M1(\Delta; {}^4S'_S) \\ &= -\frac{k}{2m} \frac{1}{\sqrt{4\pi}} F_{0010}^{2S}(00|j_0|10) \cdot (\text{isospin part}). \end{aligned} \quad (4-1)$$

From this, after taking into account the sign of the pion matrix element (see Table 6 in Appendix B), we observe that the signs of the transitions for $N(1440)$ and $\Delta(1600)$ are different. This fact is correctly shown in Tables 4 and 5. In literatures, however, the signs of the two matrix elements are found to be the same [29, 32].

4.1 Diagonalization of the $1/2^+$ states

In the DOQ model, the two $1/2^+$ states for the nucleon and the Roper, ${}^2S'_S(N = 2)$ and ${}^2S_S(N = 0)$ are not orthogonal to each other, since they are eigenstates of different Hamiltonians with different deformation: $d = 1$ and 3. Generally, those states with the same spin parity j^P but with different N are not orthogonal. Explicitly, denoting $|{}^2S'_S(N = 2)\rangle, |{}^2S_S(N = 0)\rangle \equiv |2\rangle, |0\rangle$, they have non-zero overlap

$$\langle 0|2\rangle \sim F_{0000}^{2S} \equiv \varepsilon. \quad (4-2)$$

In other words, the two states $|0\rangle$ and $|2\rangle$ form a non-orthogonal basis. Hence we need to reconstruct orthonormal basis.

Using the non-orthogonal states $|0\rangle$ and $|2\rangle$, the eigenvalue equation takes the following 2×2 matrix form:

$$(H - EN)\Psi = 0, \quad (4-3)$$

where

$$H = \begin{pmatrix} E_0 & \varepsilon E_{02} \\ \varepsilon E_{02} & E_2 \end{pmatrix}, \quad N = \begin{pmatrix} 1 & \varepsilon \\ \varepsilon & 1 \end{pmatrix}, \quad \Psi = \begin{pmatrix} a|0\rangle \\ b|2\rangle \end{pmatrix} \equiv \begin{pmatrix} a \\ b \end{pmatrix}. \quad (4-4)$$

Here the diagonal components of the energy matrix are given by (2-10):

$$E_N = \langle N|H|N\rangle = E_N^{int} - \frac{1}{2\mathcal{I}_N} \langle l^2 \rangle_N, \quad (4-5)$$

while the off diagonal components are, for simplicity, taken as the left-right average: $E_{02} = \langle 0|H|2\rangle = (E_0 + E_2)/2$. Eigenvalues and the corresponding eigenstates are given by

$$E_{N,R} = E_0 \mp (\gamma - 1)\Delta, \quad (4-6)$$

and

$$\begin{aligned} |N\rangle &= \frac{-1}{\sqrt{2(1 - \sqrt{1 - \varepsilon^2})}} (\varepsilon\gamma|0\rangle + (1 - \gamma)|2\rangle), \\ |R\rangle &= \frac{-1}{\sqrt{2(1 + \sqrt{1 - \varepsilon^2})}} (-\varepsilon\gamma|0\rangle + (1 + \gamma)|2\rangle). \end{aligned} \quad (4-7)$$

where $\gamma = 1/\sqrt{1 - \varepsilon^2}$, $\Delta = (E_2 - E_0)/2$. Numerical values for eigenvalues in units of ω are

$$E_0 = 3.0, \quad E_2 = 3.751, \quad \varepsilon = -0.538, \quad (4-8)$$

and therefore, we find

$$E_N = 2.930, \quad E_R = 3.821. \quad (4-9)$$

As expected, the mass of the nucleon is lowered and the mass of the Roper is pushed up, where the order of the effect can be estimated as

$$\frac{(E_R - E_N) - (E_2 - E_0)}{E_2 - E_0} = \frac{0.140}{0.891} = 0.157.$$

We find that the effect on the mass difference is of order ε^2 . In contrast, the wave functions (orthonormal states) are modified substantially:

$$\begin{aligned} |N\rangle &= +1.139|0\rangle + 0.332|2\rangle, \\ |R\rangle &= +0.332|0\rangle + 1.139|2\rangle. \end{aligned} \quad (4-10)$$

Using the wave functions (4-7), transition amplitudes are modified as

$$\langle R|\mathcal{M}|N\rangle = -\text{sgn}(\varepsilon) \frac{1}{1 - \varepsilon^2} \langle 0|\mathcal{M}|2\rangle + \frac{|\varepsilon|}{2(1 - \varepsilon^2)} (\langle 0|\mathcal{M}|0\rangle + \langle 2|\mathcal{M}|2\rangle). \quad (4-11)$$

Before the diagonalization only the first term with the unit coefficient ($\varepsilon \rightarrow -0$) contribute. The new terms, the second and the third terms, have the opposite sign to the first term, and therefore, the effect of the diagonalization is to reduce the amplitude. Substituting numerical numbers for the ε and matrix elements, we obtain

$$\begin{aligned} A_{1/2}^p &= 153 - 60 - 57 = 36 \text{ GeV}^{-1/2}, \\ A_{1/2}^n &= -102 + 40 + 38 = -24 \text{ GeV}^{-1/2}. \end{aligned} \quad (4-12)$$

We see that the diagonalization affects more on transition amplitudes than on masses. This is not surprising, since the effect is of order ε^2 for masses, while it is of order of ε^1 for transitions. We note that the modified values (4-12) are now rather close to those of $d = 1$.

4.2 Relativistic effects

The importance of relativistic effects was first emphasized by Kubota and Ohta already twenty years ago [33]. Further extensive studies were also performed by Capstick and Keister [29, 34]. It should be particularly so for transitions where the leading order contributions in the long wave length limit are forbidden due to some trivial selection rules. The M1 transition to the Roper resonance is a typical example of such; the M1 operator with a spin flip leaves the spatial wave function unaffected and therefore the matrix element vanishes due to the orthogonality between the initial and final spatial wave functions in the limit of zero momentum transfer, $k \rightarrow 0$. Hence the non-zero matrix element at finite k is of order $\mathcal{O}(k)$ where the relativistic corrections start to occur.

So far the fully relativistic treatment has not been achieved yet, since it inevitably requires field theoretical method for interacting light quarks. In literatures, instead, a classical method of $1/m$ expansion has been often considered [29, 32, 33, 34, 35]. We should note that this method suffers from a fundamental question whether $1/m$ expansion converges or not, when $m \sim 300$ MeV and $q \sim 500$ MeV. Although there is such a difficulty, still we think that the leading correction provides us with some flavor how relativistic effects appear.

The leading order contribution of the electromagnetic hamiltonian

$$H_\gamma = -e \int d^3x \bar{\psi} \vec{\gamma} \psi \cdot \vec{A}, \quad (4-13)$$

leads to the standard form of (3-10). The next to leading order term is of our concern here. There are two terms which are so called spin-orbit and non-additive terms. Here we consider the spin-orbit contributions in order to see the importance of relativistic corrections. Performing the Foldy-Wouthuysen transformation up to order $1/m^2$, we find the relevant terms:

$$H_\gamma \sim \frac{e}{2m} u_f^\dagger \left(-2\vec{A} \cdot \vec{p} - i\vec{\sigma} \cdot \vec{k} \times \vec{A} \right) u_i + \frac{ike}{8m^2} u_f^\dagger \left(\vec{\sigma} \cdot \vec{k} \times \vec{A} - 2\vec{\sigma} \cdot \vec{A} \times \vec{p} \right) u_i. \quad (4-14)$$

Here \vec{k} is the photon momentum and \vec{p} the momentum of the initial nucleon (acting on u_i). In deriving (4-14), we have used the condition for the real photon $\vec{k} \cdot \vec{A} = 0$.

These relativistic corrections are computed using $m \sim 300$ MeV in the DOQ model after the diagonalization is performed. We find, after including the corrections, the total amplitudes:

$$\begin{aligned} A_{1/2}^p &= -13 \times 10^{-3} \text{ GeV}^{-1/2}, \\ A_{1/2}^n &= 9 \times 10^{-3} \text{ GeV}^{-1/2}. \end{aligned} \quad (4-15)$$

As in previous works, we find that also in the DOQ model the relativistic correction changes the sign of the amplitudes. Although the DOQ values in (4-15) are larger than those of the traditional quark model, they are still too small as compared with experimental values. We note the similarity in the behaviors of the numbers in the conventional and the DOQ models when relativistic effects are included. In both cases, relativistic corrections are very large. If so, there is an essential question on the validity of the $1/m$ expansion. This is a very important problem for the non-relativistic quark model, although the model seems to work well for many phenomenological aspects. .

4.3 Limits in a non-relativistic treatment

Here, focusing on the electromagnetic transition of the Roper, we demonstrate that within a non-relativistic treatment of a naive quark model it is not possible to solve the sign problem of the amplitude. Although the statement is rather trivial, it is useful to point it out here.

As emphasized in the preceding discussions, we need to compute both the electromagnetic and the strong (pion) couplings when discussing the sign. To leading order in the non-relativistic expansion, transition operators for these two couplings are given by (3-10) and (B-4). Let us assume, as in the naive quark model, that both the nucleon and the Roper is dominated by the orbital wave function of $l = 0$: $|N\rangle \sim |\text{Roper} \equiv R\rangle \sim |[0, 1/2]^{1/2}\rangle$. Then, it is not difficult to show that both the couplings contain the spin matrix element $\langle\sigma\rangle$:

$$\langle N|H_\pi|R\rangle \cdot \langle R|H_\gamma|N\rangle \sim \langle N||\sigma||R\rangle \cdot \langle R||\sigma||N\rangle \sim |\langle N||\sigma||R\rangle|^2.$$

Therefore, it is apparent that within this treatment the sign of the amplitude can not be changed. We need more delicate treatment for a better understanding of transition amplitudes.

5 Summary

In this paper we have studied electromagnetic transitions of excited baryons using a non-relativistic quark model with a possibility for excited baryon being deformed. The main purpose of the present work is to test the success of the deformed oscillator quark (DOQ) model for the masses of flavor $SU(3)$ baryons by examining electromagnetic transitions. Experimentally, transitions from the ground state have been observed in pion photoproductions.

We have derived all necessary formulae for multipole amplitudes, which are transformed into the conventional helicity amplitudes. In the comparison of the theoretical amplitudes with experimental data, we have paid a special attention to relative signs among amplitudes by computing the pion couplings explicitly.

Our main interest is how electromagnetic amplitudes are influenced by the spatial deformation. We have seen, however, rather small dependence on deformation, which is typically less than 50 %. To this order, there are many other effects which modifies theoretical predictions. Furthermore, experimental amplitudes usually contain even larger ambiguities due to difficulties in the analysis. Other types of transitions might be useful to investigate. They could be transitions between excited states through photon or pion emission.

Another interest has been paid to the transition to the Roper resonance. The discrepancy between theoretical predictions and experimental data both in magnitude and sign should be considered seriously. It does not seem that there is a simple explanation so far, if we recall the success of the magnetic moments for the ground states of the nucleon and delta. Further investigations for the Roper resonance will be an interesting subject.

Appendix

A Helicity formalism

Empirical amplitudes for the pion photoproduction is presented by the helicity coefficients $C_\lambda^{l\pm}$ of (3-3) and (3-4). In order to compute them we explore basic ingredients for the helicity formalism, following the classic paper by Jacob and Wick [19]. Let us assume that the relative momentum between the initial photon and the nucleon is along the z -axis with their helicities being λ_γ and λ_i . In the center of mass system, the total helicity is given by $\lambda = \lambda_\gamma - \lambda_i$. This is equivalent to the z component of the angular momentum in the spherical basis. Let us write the initial state as

$$|k, \theta\phi, \lambda\rangle = |k, 00, \lambda\rangle, \quad (\text{A-1})$$

where $\theta\phi = 00$ are the polar angles of the momentum \vec{k} . Similarly we write the final state for the pion and nucleon system as

$$|q, \theta\phi, \mu\rangle, \quad (\text{A-2})$$

where $\theta\phi$ are the scattering angles of the pion, and μ is the helicity of the final state.

The helicity states (A-1) and (A-2) can be related to the spherical states through

$$|p, \theta\phi, \lambda\rangle = \sum_{jm} \sqrt{\frac{2j+1}{4\pi}} D_{m\lambda}^j(\phi, \theta, -\phi) |p, jm, \lambda\rangle, \quad (\text{A-3})$$

and the inverse relation

$$|p, jm, \lambda\rangle = \sqrt{\frac{2j+1}{4\pi}} \int d\Omega D_{m\lambda}^{j*}(\phi, \theta, -\phi) |p, \theta\phi, \lambda\rangle. \quad (\text{A-4})$$

In these equations, $D_{mn}^j(\alpha, \beta, \gamma)$ are the Wigner's D -function [22]. For rotation of a vector, the angle γ is redundant and can be fixed as $\alpha = -\gamma \equiv \phi$. The integral measure is then given by $d\Omega = d(\cos\theta)d\phi$, and so $\int d\Omega = 4\pi$.

Applying (A-3) to (A-1) and (A-2), we can rewrite the helicity amplitude (3-2)

$$\begin{aligned} A_{\mu\lambda}(\theta\phi) &\equiv \langle q, \theta\phi, \mu | \mathcal{A} | k, 00, \lambda \rangle \\ &= \sum_{jj'm} \sqrt{\frac{2j'+1}{4\pi}} \sqrt{\frac{2j+1}{4\pi}} D_{m\mu}^{j*}(\phi, \theta, -\phi) \langle q, jm, \mu | \mathcal{A} | k, j'\lambda, \lambda \rangle. \end{aligned} \quad (\text{A-5})$$

On account of the conservation of angular momentum, $j' = j$ and $m = \lambda$, we obtain

$$\langle q, \theta\phi, \mu | \mathcal{A} | k, 00, \lambda \rangle = \frac{1}{4\pi} \sum_j (2j+1) D_{\lambda\mu}^{j*}(\phi, \theta, -\phi) \langle q, j\lambda, \mu | \mathcal{A} | k, j\lambda, \lambda \rangle, \quad (\text{A-6})$$

which corresponds to (3-2).

It is instructive to re-express these relations using spherical harmonics. For this we consider

$$|k, 00, \lambda = 1/2\rangle \sim e^{i\vec{k}\cdot\vec{x}} \chi_{1/2} = 4\pi \sum_{l_\pi m_\pi} i^{l_\pi} Y_{l_\pi m_\pi}(\hat{x}) Y_{l_\pi m_\pi}^*(\hat{k}) j_{l_\pi}(kr) \chi_{1/2}, \quad (\text{A-7})$$

where $\chi_{1/2}$ is the spin up state for the nucleon. Using $Y_{l_\pi m_\pi}^*(\hat{k} = \hat{z}) = \sqrt{(2l_\pi + 1)/4\pi} \delta_{m_\pi 0}$ and recoupling the angular momentum, we find

$$|k, 00, 1/2\rangle \sim \sqrt{2\pi} \sum_j \sqrt{2j+1} \left(i^{j-1/2} \mathcal{Y}_{j1/2}^{j-1/2} - i^{j+1/2} \mathcal{Y}_{j1/2}^{j+1/2} \right), \quad (\text{A-8})$$

where $\mathcal{Y}_{jm}^{l_\pi}$ is the spinor harmonics including the spherical Bessel functions $j_{l_\pi}(kr)$:

$$\mathcal{Y}_{jm}^{l_\pi} = \sum_\mu (l_\pi \ m - \mu \ 1/2 \ \mu \ | \ j \ m) \mathcal{Y}_{l_\pi \ m - \mu} \chi_\mu, \quad (\text{A-9})$$

where $\mathcal{Y}_{lm} = Y_{lm} j_l(kr)$. Similarly, we find

$$|k, 00, -1/2\rangle \sim \sqrt{2\pi} \sum_j \sqrt{2j+1} \left(i^{j-1/2} \mathcal{Y}_{j1/2}^{j-1/2} + i^{j+1/2} \mathcal{Y}_{j1/2}^{j+1/2} \right). \quad (\text{A-10})$$

The states with a definite angular momentum can be obtained by applying the projection operator:

$$\begin{aligned} |k, jm, \pm 1/2\rangle &\sim \sqrt{\frac{2j+1}{4\pi}} \int d\Omega D_{m \pm 1/2}^{j*}(\phi, \theta, -\phi) R(\phi, \theta, -\phi) |k, 00, \pm 1/2\rangle \\ &= \frac{4\pi}{\sqrt{2}} \left(i^{j-1/2} \mathcal{Y}_{j1/2}^{j-1/2} \mp i^{j+1/2} \mathcal{Y}_{j1/2}^{j+1/2} \right). \end{aligned} \quad (\text{A-11})$$

Here $R(\phi, \theta, -\phi) = \exp(-i\alpha J_z) \exp(-i\beta J_y) \exp(-i\gamma J_z)$ is the rotation operator, and in deriving the second equation we have used the definition of the D -functions. Obviously, in these states (A-11) parities are mixed. States with a definite parity can be obtained by

$$|p, jm, \pm\rangle = \frac{1}{\sqrt{2}} (|p, jm, +1/2\rangle \pm |p, jm, -1/2\rangle) = \pm 4\pi i^{j \mp 1/2} \mathcal{Y}_{jm}^{j \mp 1/2}. \quad (\text{A-12})$$

These are the eigenstates of parity $P = \eta(-)^{l_\pi} = \eta(-)^{j \mp 1/2}$, where η is the intrinsic parity of the system.

B The pion matrix element and the sign ϵ

Let us start with the relation (3-6):

$$A_\lambda^{jP} = -i \left(\frac{1}{(2j+1)\pi} \frac{k}{q} \frac{M}{M^*} \frac{\Gamma_\pi}{\Gamma^2} \right)^{-1/2} C_\lambda^{l_\pi \pm}(M^*) C_{\pi N} \quad (\text{B-1})$$

$$= (\cdots) \langle q, j\lambda, \pm | H_\pi | N^*(j\lambda) \rangle G_j^{N^*} \langle N^*(j\lambda) | H_\gamma | k, j\lambda, \lambda \rangle C_{\pi N}. \quad (\text{B-2})$$

We need to compute the pion matrix element $\langle q, j\lambda, \pm | H_\pi | N^*(j\lambda) \rangle$ in order to account for the sign of the whole amplitude.

To do so, it is convenient to have an explicit form for the final state as given in (A-12):

$$\begin{aligned} \langle q, j\lambda, \pm | &= \left(\pm i^{l_\pi} |\mathcal{Y}_{j\lambda}^{l_\pi}\rangle \right)^\dagger = \left(\pm i^{l_\pi} \sum_m (l_\pi \ m \ 1/2 \ \lambda \ | \ -m \ j) \mathcal{Y}_{l_\pi m} |\chi_{\lambda-m}\rangle \right)^\dagger \\ &= \pm (-i)^{l_\pi} \sum_m (l_\pi \ -m \ 1/2 \ \lambda + m \ | \ j \ \lambda) (-)^m \langle \chi_{\lambda+m} | \mathcal{Y}_{l_\pi m}. \end{aligned} \quad (\text{B-3})$$

In this equation, $l_\pi \equiv j \mp 1/2$ is the orbital angular momentum for the pion relative to the nucleon. The interaction hamiltonian for the pion-quark coupling is given by

$$H_\pi = -\frac{g}{2m}\vec{\sigma}\cdot\vec{\nabla}_\pi, \quad (\text{B-4})$$

where the derivative ∇_π operates to the pion wave function. Sandwiching this hamiltonian with (B-3) and the resonance state $|N^*(j\lambda)\rangle$, we find after some algebra

$$\begin{aligned} & \langle q, j\lambda, \pm | H_\pi | N^*(j\lambda) \rangle \\ &= \mp 4\pi \frac{gq}{2m} i^{l_\pi} \left(\sqrt{\frac{l_\pi+1}{2l_\pi+1}} \langle 1/2 || [\mathcal{Y}_{l_\pi+1}\sigma]^{l_\pi} || j \rangle + \sqrt{\frac{l_\pi}{2l_\pi+1}} \langle 1/2 || [\mathcal{Y}_{l_\pi-1}\sigma]^{l_\pi} || j \rangle \right). \end{aligned} \quad (\text{B-5})$$

In fact, one of the two terms is relevant depending on the orbital angular momentum $l_q \equiv l$ of an excited quark in N^* . Due to the pseudoscalar nature of the pion-quark coupling, it follows that $l = l_\pi \pm 1$. When $j = l - 1/2$ or $j = l - 3/2$, the first term of (B-5) survives, while when $j = l + 3/2$ or $j = l + 1/2$, the second term does.

For later convenience when performing actual computations, we summarize relevant pion matrix elements according to $j = l + 3/2, l + 1/2, l - 1/2, l - 3/2$:

1. When $j = l + 3/2, l + 1/2 \xrightarrow{l_\pi=l+1} j = l_\pi \pm 1/2$,

$$\langle q, j\lambda \pm | H_\pi | N^*(j\lambda) \rangle = \mp 4\pi \frac{gq}{2m} i^{l+1} \sqrt{\frac{l+1}{2l+3}} \langle 1/2 || [\mathcal{Y}_l\sigma]^{l+1} || j \rangle. \quad (\text{B-6})$$

2. When $j = l - 1/2, l - 3/2 \xrightarrow{l_\pi=l-1} j = l_\pi \pm 1/2$,

$$\langle q, j\lambda \pm | H_\pi | N^*(j\lambda) \rangle = \pm 4\pi \frac{gq}{2m} i^{l+1} \sqrt{\frac{l}{2l-1}} \langle 1/2 || [\mathcal{Y}_l\sigma]^{l-1} || j \rangle. \quad (\text{B-7})$$

Writing the pion matrix element as

$$\langle q, j\lambda \pm | H_\pi | N^*(j\lambda) \rangle \equiv -i(-i)^l \epsilon |\langle q, j\lambda \pm | H_\pi | N^*(j\lambda) \rangle|, \quad (\text{B-8})$$

the sign ϵ is given as summarized in Table 6. In the table, η is the sign of the radial integral $\sum_n F_{00nl}^{N\sigma}(00|j_l|nl)$. The notations of this equation is defined in (C-4).

Table 6: The sign ϵ extracted from the pion matrix elements.

Nucleon			Delta		
	j	ϵ		j	ϵ
$S = 1/2$	$l + 1/2$	$-\eta_S \text{ or } \lambda$	$S = 1/2$	$l + 1/2$	$+\eta_\lambda$
	$l - 1/2$	$+\eta_S \text{ or } \lambda$		$l - 1/2$	$-\eta_\lambda$
$S = 3/2$	$l + 3/2$	$+\eta_\lambda$	$S = 3/2$	$l + 3/2$	$+\eta_S$
	$l + 1/2$	$-\eta_\lambda$		$l + 1/2$	$-\eta_S$
	$l - 1/2$	$-\eta_\lambda$		$l - 1/2$	$-\eta_S$
	$l - 3/2$	$+\eta_\lambda$		$l - 3/2$	$+\eta_S$
$\eta_\sigma \equiv \text{sgn} \left[\sum_n F_{00nl}^{N\sigma}(00 j_l nl) \right]$					

C Computation of multipole amplitudes

Using the wave functions for N^* as given in (2-22) – (2-23) one can compute multipole amplitudes in a straightforward manner. For a given excited baryon, there are three possible amplitudes: $\mathcal{M}(Ml+1)$, $\mathcal{M}(Ml-1)$ and $\mathcal{M}(El)$. To illustrate how actual computations can be performed, we consider one example for $\mathcal{M}(Ml+1)$ for the transition $|N(\text{ground state})\rangle \rightarrow |N^*; [l_S, 1/2]^j\rangle$.

In the following expressions, the factor 3 of (3-10) is not included, although it is in our numerical results. Replacing $l \rightarrow l+1$ in (3-23), only the second term survives due to the matching of orbital angular momentum. Since the initial state for the ground state nucleon is spherical, $l=0$, the orbital angular momentum of the absorbed photon and that of the excited baryon must be the same. Thus we have

$$\begin{aligned} \mathcal{M}(Ml+1) = & -\frac{k}{4m} \sqrt{\frac{l+2}{2l+3}} \left(\langle [\Psi_l^{NS} \chi^\rho]^j | [\mathcal{Y}_l \sigma]^l | \Psi_{l=0}^{0S} \chi^\rho \rangle \tau_\mu(\rho) \right. \\ & \left. + \langle [\Psi_l^{NS} \chi^\lambda]^j | [\mathcal{Y}_l \sigma]^l | \Psi_{l=0}^{0S} \chi^\lambda \rangle \tau_\mu(\lambda) \right). \end{aligned} \quad (\text{C-1})$$

Here we have included the isospin matrix elements which are defined by

$$\tau_\mu(\rho) = \langle \phi^\rho | \tau_\mu | \phi^\rho \rangle, \quad \tau_\mu(\lambda) = \langle \phi^\lambda | \tau_\mu | \phi^\lambda \rangle, \quad (\text{C-2})$$

and the radial integral $\int r^2 dr$ is implicit. Now the reduced matrix elements can be computed in a straightforward manner using the decomposition theorems, and we find the result

$$\begin{aligned} \mathcal{M}(Ml+1) = & -\frac{k}{4m} \sqrt{\frac{l+2}{2l+3}} \hat{j} \widehat{l+1} \left\{ \begin{matrix} 1/2 & j & l \\ l+1 & 1 & 1/2 \end{matrix} \right\} \\ & \times \frac{1}{4\pi} \sum_n F_{nl00}^{NS} (nl|j_l|00) \sqrt{6} \left(\tau_\mu(\rho) - \frac{1}{3} \tau_\mu(\lambda) \right), \end{aligned} \quad (\text{C-3})$$

where $\hat{l} = \sqrt{2l+1}$. Here we have introduced the notation for the radial matrix elements:

$$(nl|j_l|00) = \int r^2 dr R_{nl} j_l R_{00}, \quad (\text{C-4})$$

where R_{nl} are the radial functions of the harmonic oscillator.

All other matrix elements can be computed in similar ways. Here we summarize the results for all amplitudes. Let us introduce the following notation for the sum of the radial matrix elements:

$$P_l^{N\sigma} = \frac{1}{\sqrt{4\pi}} \sum_n F_{00nl}^{N\sigma} (nl|j_l|00), \quad (\text{C-5})$$

$$Q_l^{N\sigma} = \frac{1}{\sqrt{4\pi}} \sum_n F_{00nl}^{N\sigma} (nl'|j_l|00), \quad (\text{C-6})$$

and the combinations of isospin matrix elements

$$\begin{aligned} T_{\pm 1} &= \tau_\mu(\rho) \pm \tau_\mu(\lambda), \\ T_{\pm 1/3} &= \tau_\mu(\rho) \pm \frac{1}{3} \tau_\mu(\lambda). \end{aligned}$$

We checked the behavior of the coefficients F numerically and found that they converge to zero quickly as n is increased. In the present work, we take the sum over nine terms in (C-5) and (C-6) to obtain the accuracy of more than five digits.

The matrix elements for various excited states N^* are summarized as follows:

N1 $N^* = |[l_S, 1/2]^j\rangle$:

$$\mathcal{M}(M l + 1) = -\frac{k}{4m} \sqrt{\frac{l+2}{2l+3}} \hat{j} \widehat{l+1} \left\{ \begin{matrix} 1/2 & j & l \\ l+1 & 1 & 1/2 \end{matrix} \right\} \times P_l^{NS} \sqrt{6} T_{-1/3} \quad (\text{C-7})$$

$$\mathcal{M}(M l - 1) = \frac{k}{4m} \sqrt{\frac{l-1}{2l-1}} \hat{j} \widehat{l-1} \left\{ \begin{matrix} 1/2 & j & l \\ l-1 & 1 & 1/2 \end{matrix} \right\} P_l^{NS} \sqrt{6} T_{-1/3} \quad (\text{C-8})$$

$$\mathcal{M}(El) = -\frac{\sqrt{l(l+1)}}{2m} (-1)^l \hat{j} Q_l^{NS} T_{+1} + \frac{k}{4m} \hat{j} \hat{l} \left\{ \begin{matrix} 1/2 & j & l \\ l & 1 & 1/2 \end{matrix} \right\} P_l^{NS} \sqrt{6} T_{-1/3} \quad (\text{C-9})$$

N2 $N^* = |[l_{MS}, 1/2]^j\rangle$:

This case is obtained simply by performing the following replacements in the results of (N1).

- Multiply $1/\sqrt{2}$ as an overall factor.
- Change the sign of one of the isospin matrices: $+\tau_\mu(\lambda) \rightarrow -\tau_\mu(\lambda)$.
- Replace the superscript of the coefficient F : $F_{00nl}^{NS} \rightarrow F_{00nl}^{N\lambda}$ and hence $P_l^{NS} \rightarrow P_l^{N\lambda}$ and $Q_l^{NS} \rightarrow Q_l^{N\lambda}$.

N3 $N^* = |[l_{MS}, 3/2]^j\rangle$:

$$\mathcal{M}(M l + 1) = -\frac{k}{4m} \sqrt{\frac{l+2}{2l+3}} \hat{j} \widehat{l+1} \left\{ \begin{matrix} 3/2 & j & l \\ l+1 & 1 & 1/2 \end{matrix} \right\} P_l^{N\lambda} \frac{4}{\sqrt{3}} \tau_\mu(\lambda) \quad (\text{C-10})$$

$$\mathcal{M}(M l - 1) = \frac{k}{4m} \sqrt{\frac{l-1}{2l-1}} (-1)^{j+3/2} \hat{j} \widehat{l-1} \left\{ \begin{matrix} 3/2 & j & l \\ l-1 & 1 & 1/2 \end{matrix} \right\} P_l^{N\lambda} \frac{4}{\sqrt{3}} \tau_\mu(\lambda) \quad (\text{C-11})$$

$$\mathcal{M}(El) = -\frac{k}{4m} \hat{j} \hat{l} \left\{ \begin{matrix} 3/2 & j & l \\ l & 1 & 1/2 \end{matrix} \right\} P_l^{N\lambda} \frac{4}{\sqrt{3}} \tau_\mu(\lambda) \quad (\text{C-12})$$

The decays of delta excited states $\Delta 1$ and $\Delta 2$ are obtained by the following manipulations.

$\Delta 1$ $\Delta^* = |[l_{MS}, 1/2]^j\rangle$: In the results of **N1**

- Pick up the $\tau_\mu(\lambda)$ -term and replace $\tau_\mu \rightarrow \langle \phi^\lambda | \tau_\mu | \phi^S \rangle$.
- Replace F_{00nl}^{NS} by $F_{00nl}^{N\lambda}$.

$\Delta 2$ $\Delta^* = |[l_S, 3/2]^j\rangle$: In the results of **N3**

- Replace $\tau_\mu \rightarrow \langle \phi^\lambda | \tau_\mu | \phi^S \rangle$.

- Replace F_{00nl}^{NS} by $F_{00nl}^{N\lambda}$.
- Multiply $\sqrt{2}$ as an overall factor.

For practical purposes, it is convenient to write the spin of excited baryons j by l ($j = l \pm 1/2$ or $l \pm 3/2$), so that the 6- j symbols are computed explicitly. Results are:

N1.a $N^* = |[l_S, 1/2]^{l+1/2}\rangle$, allowed transitions: $M l + 1$ and $E l$,

$$\mathcal{M}(M l + 1) = -\frac{k}{4m} \sqrt{2(l+2)} P_l^{NS} T_{-1/3} \quad (\text{C-13})$$

$$\mathcal{M}(E l) = \frac{\sqrt{2l(l+1)}}{2m} Q_l^{NS} T_{+1} + \frac{k\sqrt{2l}}{4m} P_l^{NS} T_{-1/3} \quad (\text{C-14})$$

N1.b $N^* = |[l_S, 1/2]^{l-1/2}\rangle$, allowed transitions: $M l - 1$ and $E l$,

$$\mathcal{M}(M l - 1) = \frac{k}{4m} \sqrt{2(l-1)} P_l^{NS} T_{-1/3} \quad (\text{C-15})$$

$$\mathcal{M}(E l) = -\frac{\sqrt{2(l+1)l}}{2m} Q_l^{NS} T_{+1} + \frac{k\sqrt{2(l+1)}}{4m} P_l^{NS} T_{-1/3} \quad (\text{C-16})$$

N2 The results for this case, where $N^* = |[l_S, 1/2]^{l\pm 1/2}\rangle$ are obtained by making the replacements as described before.

N3.a $N^* = |[l_{MS}, 3/2]^{l+3/2}\rangle$, allowed transitions: $M l + 1$,

$$\mathcal{M}(M l + 1) = \frac{k}{2m} \sqrt{\frac{2}{3}} \frac{l+2}{\sqrt{2l+3}} P_l^{N\lambda} \tau_\mu(\lambda) \quad (\text{C-17})$$

N3.b $N^* = |[l_{MS}, 3/2]^{l+1/2}\rangle$, allowed transitions: $M l + 1$ and $E l$,

$$\mathcal{M}(M l + 1) = -\frac{k}{3m} \sqrt{\frac{l(l+2)}{2(2l+3)}} P_l^{N\lambda} \tau_\mu(\lambda) \quad (\text{C-18})$$

$$\mathcal{M}(E l) = -\frac{k}{3m} \sqrt{\frac{2l+3}{2}} P_l^{N\lambda} \tau_\mu(\lambda) \quad (\text{C-19})$$

N3.c $N^* = |[l_{MS}, 3/2]^{l-1/2}\rangle$, allowed transitions: $M l - 1$ and $E l$,

$$\mathcal{M}(M l - 1) = -\frac{k}{3m} \sqrt{\frac{(l-1)(l+1)}{2(2l-1)}} P_l^{N\lambda} \tau_\mu(\lambda) \quad (\text{C-20})$$

$$\mathcal{M}(E l) = \frac{k}{3m} \sqrt{\frac{2l-1}{2}} P_l^{N\lambda} \tau_\mu(\lambda) \quad (\text{C-21})$$

N3.d $N^* = |[l_{MS}, 3/2]^{l-3/2}\rangle$, allowed transitions: $M l - 1$,

$$\mathcal{M}(M l - 1) = \frac{k}{2m} \sqrt{\frac{2}{3}} \frac{l-1}{\sqrt{2l-1}} P_l^{N\lambda} \tau_\mu(\lambda) \quad (\text{C-22})$$

Similarly, we can derive the formulae for deltas.

References

- [1] See, for example, *Proceedings of the CEBAF/INT workshop for N^* physics*, Ed. by T.-H. Lee and W. Roberts, World Scientific (1997).
- [2] R.K. Bhaduri, *Models of the Nucleon*, Lecture notes and supplements in physics, Addison-Wesley (1988).
- [3] N. Isgur and G. Karl, Phys. Lett. 72B (1977) 109; *ibid.* 74B (1978) 353; Phys. Rev. D18 (1978) 4187; *ibid.* D20 (1979) 1191.
- [4] R. Koniuk and N. Isgur, Phys. Rev. D21 (1980) 1868.
- [5] L.Ya. Glozman and D.O. Riska, Phys. Rept. 268 (1996) 263.
- [6] A. Hosaka, H. Toki and M. Takayama, Mod. Phys. Lett. A13 (1998) 1699
- [7] M. Takayama, H. Toki and A. Hosaka, Prog. Theor. Phys. 101 (1999) 1271.
- [8] C. Caso et al. (Particle Data Group), Euro. Phys. J. C3 (1998) 1
- [9] R.M. Barnett et al. (Particle Data Group), Phys. Rev. D54 (1996) 1.
- [10] H. Toki, J. Dey and M. Dey, Phys. Lett. B133 (1983) 20.
- [11] R.K. Bhaduri, B.K. Jennings and J.C. Wadington, Phys. Rev. D29 (1984) 2051;
M.V.N. Murthy, M. Dey, J. Dey and R.K. Bhaduri, Phys. Rev. D30 (1984) 152;
M.V.N. Murthy, M. Brack, R.K. Bhaduri and B.K. Jennings, Z. Phys. C29 (1985) 385.
- [12] R.L. Walker, Phys. Rev. 182 (1969) 1729.
- [13] R.G. Moorhouse, “*Electromagnetic excitation and decay of hadron resonances*”, in *Electromagnetic interactions of hadrons, Ch.2*, edited by A. Donnachie and G. Shaw, Plenum (1978).
- [14] Particle Data Group, Rev. Mod. Phys. 48 (1976) Part II.
- [15] A. Bohr and B. Mottelson, “Nuclear Structure”, Benjamin Inc. (1975).
- [16] M. Takayama, A. Hosaka and H. Toki, Nucl. Phys. A663&664 (2000) 695c (Proceedings of the 15th International Conference on Particle and Nuclei (PANIC 99), Uppsala, Sweden, 10-16 June, 1999).
- [17] R.E. Peierls and J. Yoccoz, Proc. Phys. Soc. London 70 (1957) 381.
- [18] P. Ring and P. Shuck, *The nuclear many body problem*, Springer, New York (1980).
- [19] M. Jacob and G.C. Wick, Ann. Phys. 7 (1959) 404.
- [20] M. Gourdin and Ph. Salin, Nov. Cim. 27 (1963) 193.
- [21] M.E. Rose *Elementary theory of angular momentum*, Wiley (1957) p131.
- [22] D.A. Varshalovich, A.N. Moskalev and V.K. Khersonskii, *Quantum Theory of Angular Momentum* World Scientific (1988).
- [23] M. Arima, K. Shimizu and K. Yazaki, Nucl. Phys. A543 (1992) 613.
- [24] R.P. Feynman, M. Kislinger and F. Ravndal, Phys. Rev. D3 (1971) 2706.

- [25] R.G. Moorhouse and N.H. Parsons, Nucl. Phys. B62 (1973) 109.
- [26] M.V.N. Murthy and R.K. Bhaduri, Phys. Rev. Lett. 54 (1985) 745.
- [27] Y.B. Dong, K. Shimizu, A. Faessler and A.J. Buchmann, Phys. Rev. C60 (1999) 035203.
- [28] U. Meyer, A.J. Buchmann, and A. Faessler Phys. Lett. B408 (1997) 19.
- [29] S. Capstick, Phys. Rev. D46 (1992) 2864.
- [30] B. Nefkens et al., Phys. Rev. D18 (1978) 3911.
- [31] T. Sato and T.-S.H. Lee, Phys. Rev. C54 (1996) 2660.
- [32] F.E. Close and Z. Li, Phys. Rev. D42 (1991) 2194.
- [33] T. Kubota and K. Ohta, Phys. Lett. B65 (1976) 374.
- [34] S. Capstick and B.D. Keister, Phys. Rev. D51 (1995) 3598.
- [35] S.J. Brodsky and J.R. Primack, Ann. Phys. 52 (1969) 315.